Hindawi
International Journal of Polymer Science
Volume 2020, Article ID 9876408, 10 pages
https://doi.org/10.1155/2020/9876408

Research Article

Synthesis, Characterization, and Properties of Sulfonated Chitosan for Protein Adsorption

Xiaomin Zhang and Jie Sun

Department of Chemical Engineering, Zhejiang Ocean University, Zhoushan, Zhejiang 316022, China

Correspondence should be addressed to Xiaomin Zhang; 1279857017@qq.com

Received 8 June 2020; Revised 19 August 2020; Accepted 26 August 2020; Published 7 September 2020

Academic Editor: Miriam H. Rafailovich

Chitosan sulfate was prepared and characterized as a new chromatography media for protein separation. The degree of sulfonation of chitosan could be well controlled and impacted under conditions in the synthesis process. The prepared chitosan sulfate shows improved binding capacity with proteins. Sulfonated chitosan shows improved ion-exchange adsorption properties with proteins, which could have good potential in protein purification.

1. Introduction

With the rapid development of monoclonal antibody (mAb) therapeutics in the past decade, such as PD-1/PD-L1 immune checkpoint inhibitors, the worldwide demand of therapeutic proteins has been increasing dramatically, which raised the production capacity of therapeutic proteins accordingly [1]. Protein purification is one of the most important stages in GMP-compliant industrial scale mAb manufacturing process, and ion-exchange chromatography plays the crucial role of capturing targeted proteins during purification processes [2–6]. It is very important in the ion-exchange chromatographic systems to use porous adsorbent particles which can provide the highest possible breakthrough capacity for the desired bioactive molecules. To enhance breakthrough capacity, it is effective to covalently link positive or negative affinity ligands/groups to extenders, and one of the suitable extenders has been found to be polysaccharides [7–12].

Chitosan, as a natural polysaccharide, has a porous structure, suitable specific surface area, and good biological affinity [13–16]. Therefore, it has been widely studied as a good candidate of an ideal extender. However, it has rarely been studied as a bioseparation media for protein purification, partially due to its poor water solubility, limiting its applications in the field of protein purification [17–20]. Furthermore, its direct interactions with proteins are to form small emulsion droplets or the formation of soluble or insoluble complexes [21], and the electrostatic effect is not very good [22] too. It has been found that improving the surface hydrophilicity of chitosan can generate accommodated sites on the surface for protein adsorption [23, 24]. Therefore, chemical modification of chitosan becomes a feasible way to improve its surface properties for protein adsorption.

Chemical modification of chitosan can change its structures and physicochemical properties [25], e.g., biocompatibility, adsorption capacity, and electrostatic properties [14, 26, 27], thus extending its applications in the biopharmaceutical industry. Shi et al. [9] took polysaccharide to synthesize a cation exchanger, similar to chitosan. Saxena et al. [24] studied the chitosan/silica composite media as a membrane used in protein separation [28]. Due to its swollen property, chitosan could easily lose its physical structure, thus making it not a good candidate as the membrane separation media. As an amino polysaccharide, chitosan is a promising hydrophilic material. Therefore, considering its hydrophilic nature and high affinity for water, chitosan-based material could have great potentials in protein separation and purification [23, 24, 29, 30].

In this paper, sulfonated chitosan has been synthesized through a well-controlled process and then characterized by FT-IR, XRD, SEM, DSC, and TGA. Its adsorption properties to proteins have been studied by using bovine serum albumin (BSA).

2. Experimental

2.1. Materials. Chitosan with a degree of deacetylation ≥95% was purchased from Shanghai Aladdin; bovine hemoglobin, bovine serum albumin (BSA), and the sulfonating agent-98% sulfuric acid, and chlorosulfonic acid were purchased from Sinopharm Chemical Reagent Co., Ltd. (Shanghai). All other chemicals and reagents are of analytical grade.

2.2. Method

2.2.1. Synthesis of Sulfonated Chitosan. Chitosan was dissolved in a diluted acetic acid solution and placed in a three-necked flask. Concentrated sulfuric acid (98%) was added into the chitosan solution dropwise with the water bath of 50°C, and the temperature was maintained for 3 hours. After the reaction was completed, the solution was poured into anhydrous ethanol at 5°C and placed overnight. Then, the solution was neutralized with ammonia, and white precipitate was obtained at pH = 7. The precipitate was washed with acetone and methanol sequentially and finally dried at 60°C afterwards.

2.3. Characterization

2.3.1. Infrared Spectroscopy (FTIR). FTIR spectra were recorded on a PerkinElmer model 1600 IR spectrometer (Nicololi, USA), operating from 4000 to 400 cm^{-1}, in a resolution of 4 cm^{-1}, obtained after cumulating of 64 scans.

2.3.2. Wide Angle X-Ray Scattering. X-ray diffraction was performed by a Rigaku 18 KW Rotating Anode X-ray Generator Xray. Diffractometer was used to investigate the solid-state morphology of sulfonated chitosan in film form (Cermet X-ray tubes, power 1200w (tube voltage 40 kV, tube current 30 mA)). X-rays with a wavelength of 1.5406A° were generated using a CuKa source. The angles were chosen as the starting angle 5°and the ending angle 50°.

2.3.3. Thermal Gravimetric Analysis. TGA was performed on the HCT-1 microcomputer differential thermobalance (Beijing) at a heating rate of 10°C/min under a nitrogen flow rate of 100 mL/min.

2.3.4. Differential Scanning Calorimetry. Integrated Thermal Analyzer was utilized to test the effect of heating on chitosan and sulfonated chitosan. The instrument used for this study is DSC200-F3 (German NETZSCH).

2.3.5. Scanning Electronic Microscopy. SEM was used to examine surface morphologies of chitosan sulfate. JSM-IT100 scanning electron microscope (Japan Electronics Corporation) with the magnification 5x-300,000x and Tungsten filament zoom spotlight is used in this study.

2.3.6. Specific Surface Area and Pore Size Analysis. Surface and pore information were obtained by using Automated Adsorption Instrument of Autosor-IQ-C-TCD (Quantachrome Corporation). Specific surface area and pore size analysis (BET) was tested at room temperature, through the nitrogen adsorption and desorption.

2.3.7. Protein Adsorption. The binding properties (capacity) of bovine serum albumin (BSA) onto sulfonated chitosan and chitosan in citric acid buffer were investigated, respectively. Experiments were performed in citric acid buffer at pH = 3. BSA was added into accurately weighed 7 parts of 0.5 g of sulfonated chitosan and chitosan in an Erlenmeyer flask and put them into a shaker thermostat at a temperature of 25°C for 24 hours. The binding behavior of BSA and the adsorption amount was measured by an ultraviolet spectrophotometer.

3. Results and Discussion

3.1. Characterization of Sulfonated Chitosan

3.1.1. FTIR. Chitosan and sulfonated chitosan were characterized by Fourier Transform Infrared Spectrometer. Figure 1 shows FTIR spectra of both chitosan and sulfonated chitosan.

It can be seen from Figure 1 that there existed the characteristic bands of the chitosan in the spectrum, including characteristic broad peaks at 3300-3400 cm^{-1} which corresponds to the hydrophilic groups in Chitosan, such as -OH and -NH2, demonstrating the strong hydrogen interactions, and at 2850 cm^{-1} which corresponds to the stretching vibration of -CH_2-, and also the absorption peaks at 1650 cm^{-1} and 1600 cm^{-1} which correspond to the stretching vibration of -NH_2- group. The peak of 1470 cm^{-1} is the deformation vibration of -CH_2-, and the peak of 1422 cm^{-1} is the associative secondary alcohol -OH deformation vibration, and also, the peak of 1345 cm^{-1} is the group -CH deformation vibration, and the peak at 1030 cm^{-1} is the primary alcohol C-O stretching vibration. The above results are consistent with the structure of chitosan.

Figure 1 also presented the FTIR spectra of sulfonated chitosan. It can be shown from Figure 1 that many characteristic peaks for chitosan sulfate existed, including the peak of 691 cm^{-1} which corresponds to N-SO_2, the strong absorption peak between 800 cm^{-1} and 813 cm^{-1} which correspond to the characteristic peaks of sulfate-based O-S and the symmetrical vibration of C-O-S, the weak peak of around 915 cm^{-1} which corresponds to parasulfamoyl, the peak at about 1034 cm^{-1} which corresponds to O-S-O stretching vibration, the peak at 1180-1270 cm^{-1} which corresponds to S=O asymmetrical stretching vibration in OSO^{3-} group, the peak at 1385 cm^{-1} which corresponds to the asymmetric stretching vibration absorption and symmetrical stretching vibration absorption of sulfate, the peak at 1419 cm^{-1} which corresponds to N-SO_2, the peak at 1525 cm^{-1} which corresponds to the bending vibration of C-N-C, and the peak at 1670 cm^{-1} (a weak peak) which corresponds to the bending vibration absorption of the NH-SO_3H group. All the above results reveal the presence of sulfonic groups in the modified chitosan.

Comparing FTIT spectra between chitosan and chitosan sulfate, it can be seen that the absorption peaks of chitosan sulfate at 3400 cm^{-1} and 1422 cm^{-1} are obviously weakened, and the disappearance of the absorption peak at 1030 cm^{-1} indicated that the primary -OH group is involved in the sulfonation reaction. The weakening of the absorption peak at

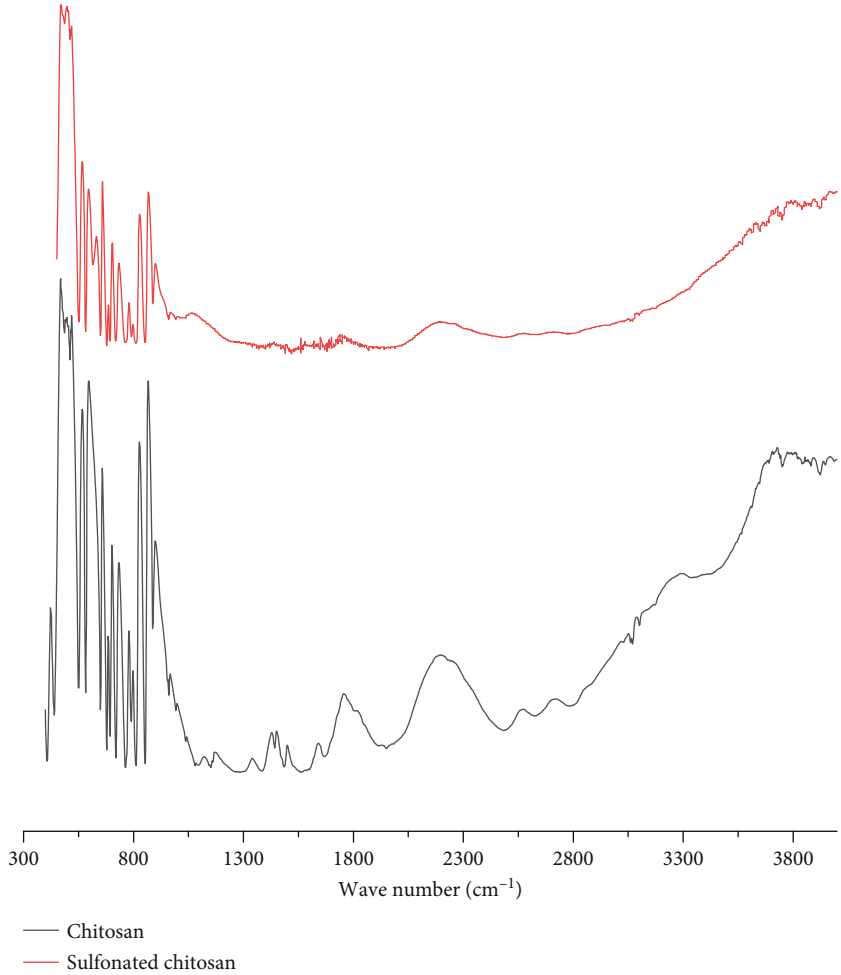

(a)

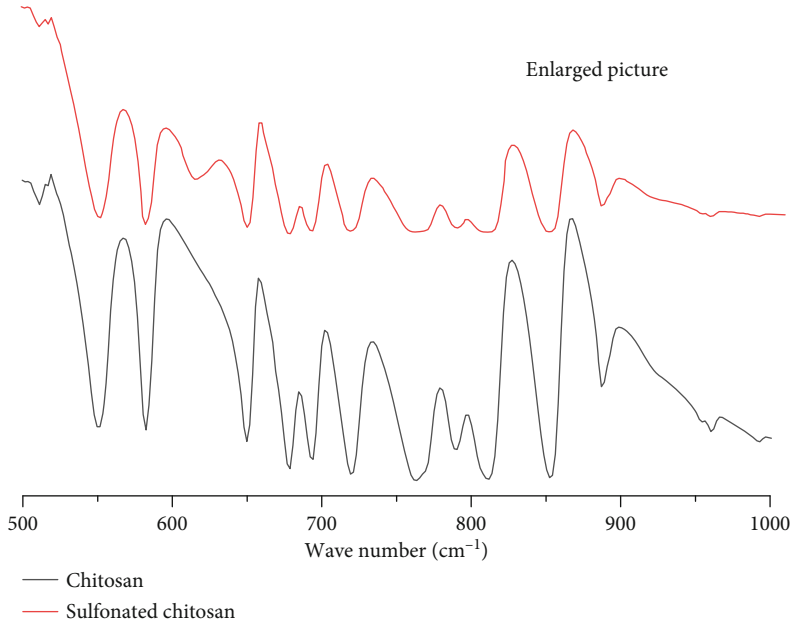

(b)

Figure 1: Continued.

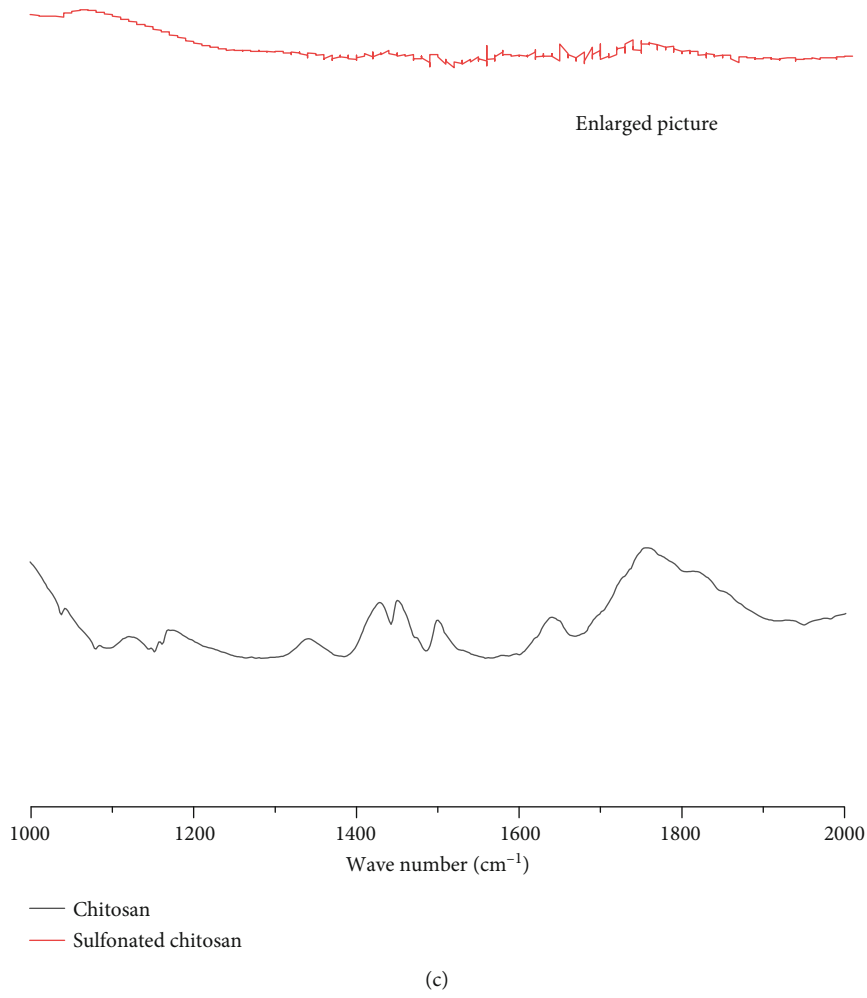

FIGURE 1: FTIR spectra of chitosan and sulfonated chitosan: (a) full spectra; (b) enlarged spectra between 500 and 1000 cm^{-1}; (c) enlarged spectra between 1000 and 2000 cm^{-1}.

2850 cm^{-1} is due to the degradation of the chitosan backbone. In addition, the FTIR spectrum of sulfonated chitosan showed numerous characteristic peaks of sulfonic acid groups, as discussed in the above paragraph. Altogether, these results demonstrate that the sulfonation reaction of chitosan was well controlled.

3.1.2. XRD Results. XRD patterns of chitosan and sulfonated chitosan are shown in Figure 2. It can be seen from Figure 2 that chitosan shows two reflections at $2\theta = 20^\circ$ and $2\theta = 12.5^\circ$, which correspond to crystal formal II and I (Samuels, 1981). The sulfonated chitosan has the peak intensity decreased at the position of $2\theta = 20^\circ$, and the peak for chitosan at $2\theta = 12.5^\circ$ has been shifted to $2\theta = 15^\circ$ for sulfonated chitosan, with deceased peak intensity, too. These results show that the sulfonation has reduced the capability to form a hydrogen bond in chitosan sulfate than those in chitosan, thus causing the decrease of the crystallinity of both chitosan crystal form II and form I. In addition, it cannot be ignored that there exist many unassigned peaks on the XRD pattern of sulfonated chitosan, which may be caused by the perturbations during XRD experimental process.

3.1.3. Thermal Analysis. Figure 3(a) shows the thermogravimetric analysis (TGA) thermograms of chitosan and sulfonated chitosan. It can be seen from Figure 3(a) that the degradation of chitosan is divided into two stages, and the degradation of sulfonated chitosan is divided into three stages. The degradation process of chitosan is divided into the dehydration stage (25-100°C) and the main chain degradation stage (250-500°C), while the degradation process of sulfonated chitosan is divided into three stages: the dehydration stage (25-100°C), the sulfuric acid group degradation stage (100-250°C), and the main chain degradation stage (250-500°C). Therefore, these results clearly show that the sulfonic group has been successfully incorporated into chitosan sulfate.

Figure 3(b) shows the differential thermal analysis (DTA) thermograms of both chitosan and sulfonated chitosan. It can be seen from Figure 3(b) that the DTA thermograms of the two materials are quite different. The endotherm of chitosan at 100°C is due to the evaporation of water of crystallization. A strong exotherm peak at about 300°C is due to the decomposition of amine groups (GlcN, see Figure 3(c)) in chitosan [31]. The DTA results of chitosan sulfate show that

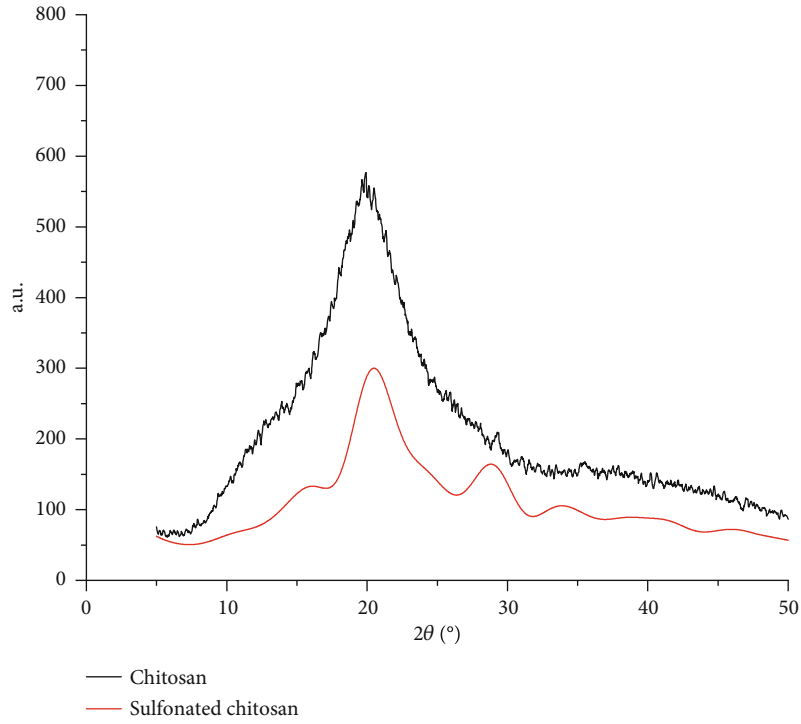

Figure 2: XRD patterns of chitosan and sulfonated chitosan.

at a temperature of 100°C, the oscillation amplitude for sulfonated chitosan is less than that of chitosan, which indicates that the absorbed crystallization heat of sulfonated chitosan is significantly less than that of chitosan. Also, strong endothermic peaks appear at 325°C and 400°C, respectively, which correspond to the two major degradations of the materials.

3.1.4. SEM. Figure 4 shows the SEM micrographs of both chitosan and sulfonated chitosan. It can be seen from Figure 4 that the surface of chitosan (Figure 4(a)) itself is porous and has a large specific surface area, and the surface of sulfonated chitosan (Figure 4(b)) is more rougher and more porous than those of chitosan, which due to the sulfonic group to reduce the cross-linking density, thus increasing the capacity to holding water.

3.1.5. BET. The specific surface area of the sulfonated chitosan was obtained by adsorption and desorption measurements based on nitrogen adsorption by BET and Langmuir methods, as is shown in Figure 5. It can be found that the specific surface area obtained by the BET method is 17.20123 m^2/g, whereas the specific surface area obtained by the Langmuir method is 25.26701 m^2/g. Since the Langmuir method assumes a single layer adsorption, there is a certain gap between the actual adsorption conditions of the material and the hypothesis, so the BET method could be more accurate to reflect the actual specific surface area. If it is protein adsorption, considering the single layer adsorption, the Langmuir method can better represent the actual surface area. In addition, the Langmuir adsorption isotherm of the sulfonated chitosan is a type III isotherm. The amount of adsorption in the low-pressure zone is relatively small, and the forces between sulfonated chitosan and nitrogen are relatively weak.

From Figure 6, it has been shown that the majority of pores are within the ten nanometers, which is the suitable size for protein transportation and adsorption onto the internal surfaces of sulfonated chitosan. It can be also shown from Figure 6 that the distribution of the pore size is mainly limited in the range of micropores and mesopores, which is adaptable to general protein size to provide channels for protein intraparticle transportation and further adsorption onto intraparticle internal surfaces. Moreover, these intraparticle pores increase the pore volume for the ion exchange ligands to be located inside, thus further improving protein adsorption onto the ligands. Therefore, this new sulfonated chitosan material could have great potential for applications in protein adsorption.

3.1.6. Optimization of Reaction Conditions. It should be noted that there exist optimal reaction conditions to control the degree of sulfonation of chitosan. The conditions include sulfonating reagent, sulfonation auxiliary reagent, neutralizing reagent, reaction time, and reaction temperature. By changing these conditions, the degree of sulfonation of chitosan can be well controlled, and these conditions could be called optimal reaction conditions. This work has tremendous experiments, and it is suitable to be depicted in other place.

3.2. Binding Activity. Macromolecular interaction between polysaccharides and proteins could always be observed through the phenomena of flocculation formation in the

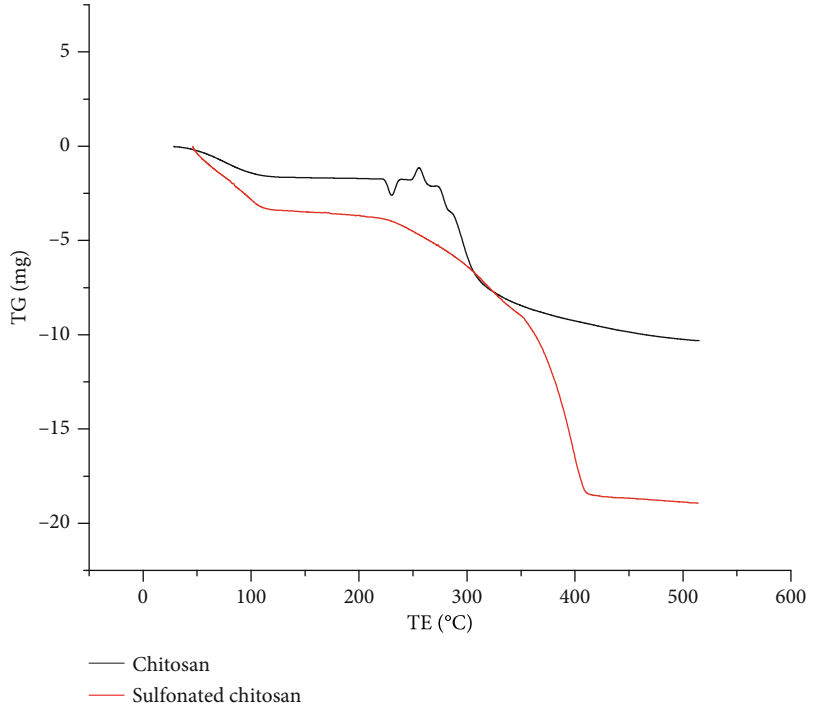

(a)

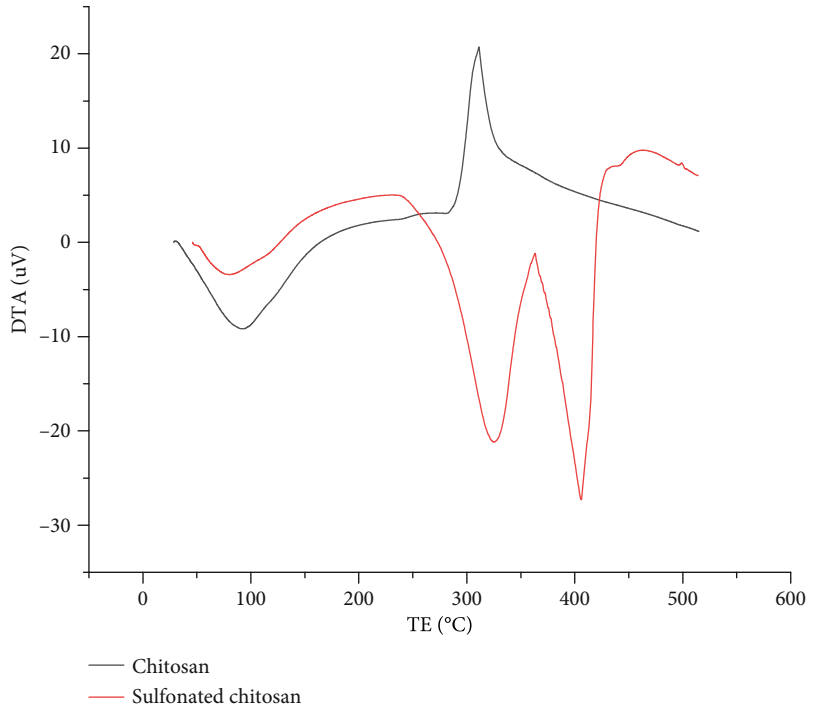

(b)

Figure 3: Continued.

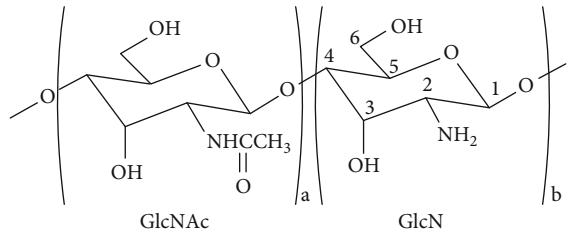

(c)

Figure 3: (a) TGA and (b) DTA thermograms of chitosan and sulfonated chitosan. (c) Structural formula for GIcN and GIcNAc.

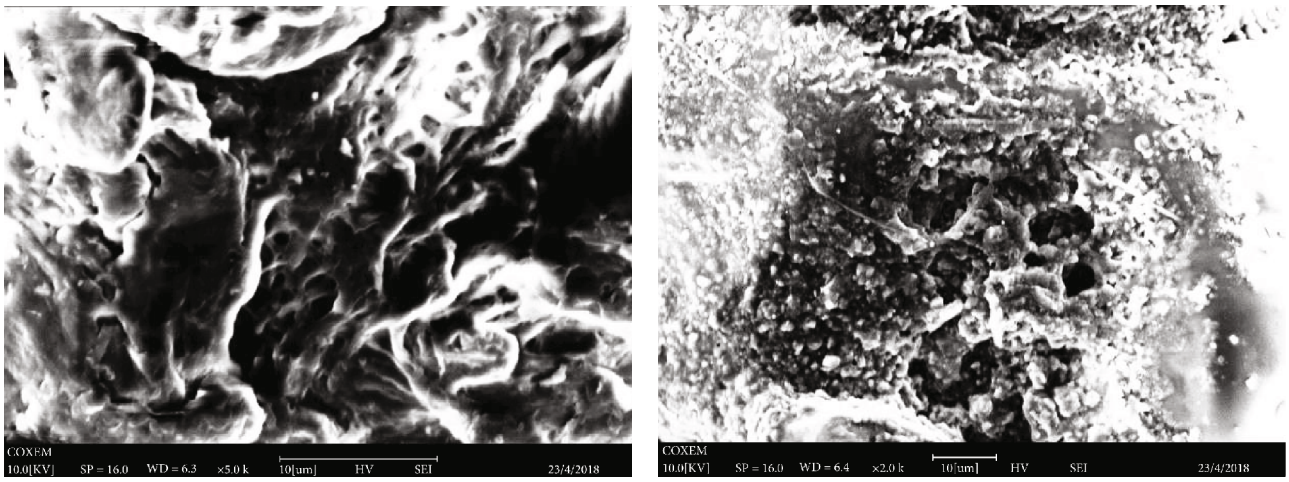

(a) (b)

Figure 4: Scanning electron micrographs of chitosan (left) and sulfonated chitosan (right).

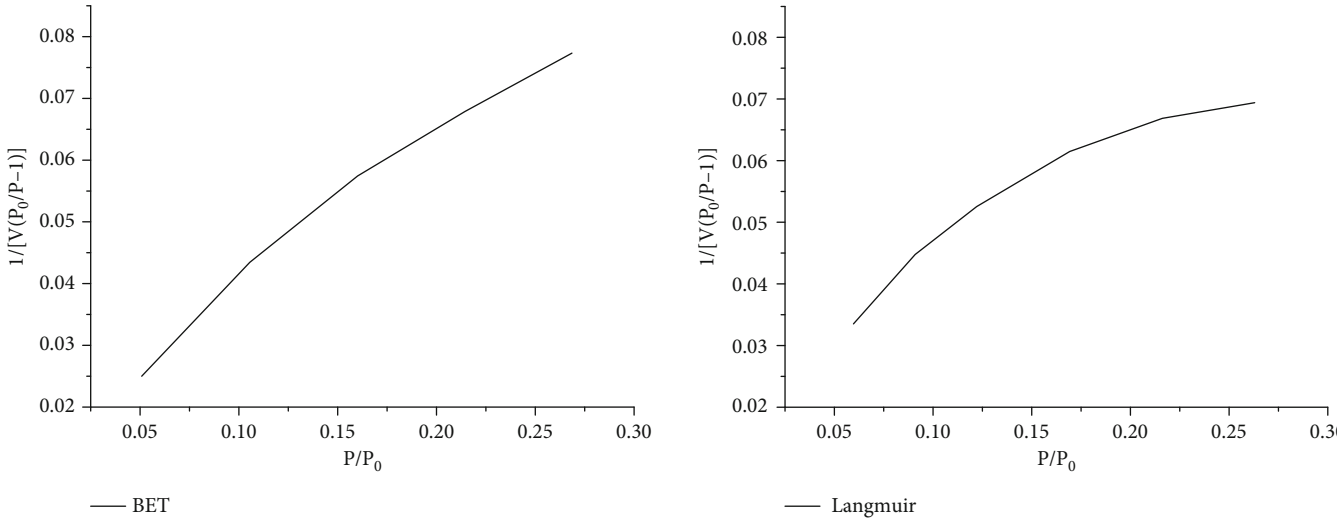

Figure 5: Specific surface area measured by BET method and Langmuir method.

solutions. In this case, the binding behaviors of BSA with both sulfonated chitosan and native chitosan were examined. It was clearly shown in Figure 7 that the binding amounts of BSA onto sulfonated chitosan and onto chitosan are quite different. The enhancement of protein binding is originated from the sulfonation of chitosan. The possible mechanism is that the introduction of sulfate groups on chitosan chains increases the negative charges, and BSA, as a polyelectrolyte, exhibits partial charges on multiple points on protein structures, which enhance the capability to interact with the ulfate group, thus improving its binding capacity onto sulfonated chitosan.

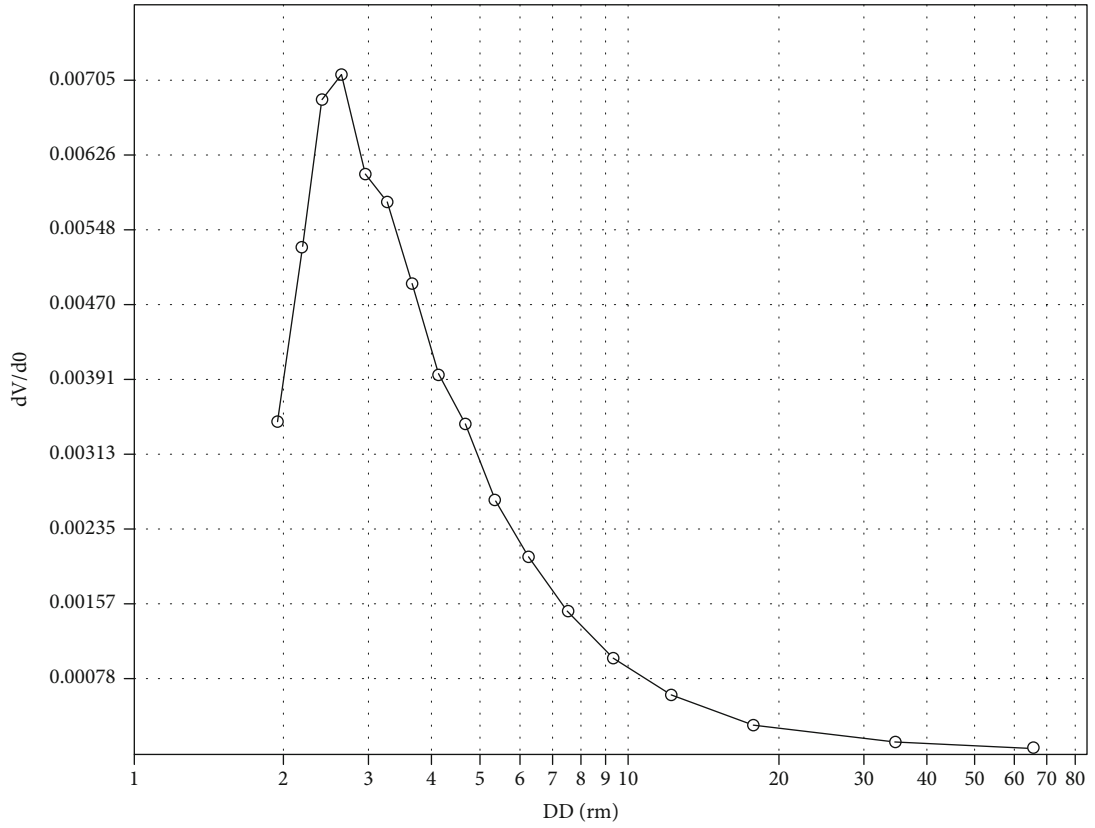

Figure 6: Distribution of pore size and pore volume.

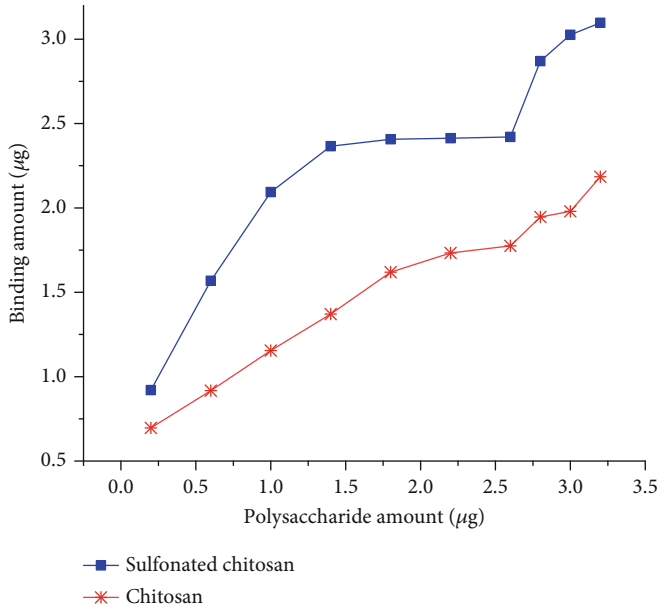

Figure 7: The binding capacity of BSA on sulfonated chitosan and chitosan.

4. Conclusions

Sulfonated chitosan was prepared and well characterized by FTIR, TGA/DTA, XRD, SEM, and BET/Langmuir. The results show that sulfonic groups have been successfully incorporated into chitosan. The ionic exchange adsorption properties of the prepared chitosan sulfate to BSA show remarkable improvements than those of chitosan. Sulfonated chitosan has great potential to be used in the ion-exchange separation process of protein purification as a new chromatography media.

Data Availability

The data used to support the findings of this study are included within the article.

Conflicts of Interest

The authors declare that they have no conflicts of interests.

Acknowledgments

This work is supported by the Zhoushan Scientific and Technological Program (No. 2017C41020).

References

[1] G. Walsh, "Biopharmaceutical benchmarks 2006," *Nature Biotechnology*, vol. 24, no. 7, pp. 769–776, 2006.

[2] X. Zhang, B. A. Grimes, J. C. Wang, K. M. Lacki, and A. I. Liapis, "Analysis and parametric sensitivity of the behavior of overshoots in the concentration of a charged adsorbate in the adsorbed phase of charged adsorbent particles: practical implications for separations of charged solutes," *Interface Science*, vol. 273, no. 1, pp. 22–38, 2004.

[3] A. M. Lenhoff, "Ion-exchange chromatography of proteins: the inside story," *Materials Today: Proceedings*, vol. 3, no. 10, pp. 3559–3567, 2016.

[4] C. Q. Gu, J. W. Li, F. Chao, M. Jin, X. W. Wang, and Z. Q. Shen, "Isolation, identification and function of a novel anti-HSV-1 protein from Grifola frondosa," *Antiviral Research*, vol. 75, no. 3, pp. 250–257, 2007.

[5] M. Salvalaglio, M. Paloni, B. Guelat, M. Morbidelli, and C. Cavallotti, "A two level hierarchical model of protein retention in ion exchange chromatography," *Journal of Chromatography A*, vol. 1411, pp. 50–62, 2015.

[6] T. Ishihara, T. Kadoya, N. Endo, and S. Yamamoto, "Optimization of elution salt concentration in stepwise elution of protein chromatography using linear gradient elution data," *Journal of Chromatography. A*, vol. 1114, no. 1, pp. 97–101, 2006.

[7] E. Boschetti, J. L. Coffman, and G. Subramanian, *Bioseparation and Bioprocessing: Biochromatography, Membrane Separations, Modeling, Validation*, Wiley-VCH, Weinheim, 1998.

[8] Y. Wang, X. Zhang, N. Han, Y. Wu, and D. Wei, "Oriented covalent immobilization of recombinant protein A on the glutaraldehyde activated agarose support," *International Journal of Biological Macromolecules*, vol. 120, Part A, pp. 100–108, 2018.

[9] Q. H. Shi, G. D. Jia, and Y. Sun, "Dextran-grafted cation exchanger based on superporous agarose gel: Adsorption isotherms, uptake kinetics and dynamic protein adsorption performance," *Journal of Chromatography. A*, vol. 1217, no. 31, pp. 5084–5091, 2010.

[10] X. Zhang, J.-C. Wang, K. M. Lacki, and A. I. Liapis, "Construction by molecular dynamics modeling and simulations of the porous structures formed by dextran polymer chains attached on the surface of the pores of a base matrix: characterization of porous structures," *The Journal of Physical Chemistry. B*, vol. 109, no. 44, pp. 21028–21039, 2005.

[11] X. Li, Q. Wang, X. Dong, Y. Liu, and Y. Sun, "Grafting glycidyl methacrylate-iminodiacetic acid conjugate to Sepharose FF for fabrication of high-capacity protein cation exchangers," *Biochemical Engineering Journal*, vol. 138, pp. 74–80, 2018.

[12] A. M. Lenhoff, "Protein adsorption and transport in polymer-functionalized ion-exchangers," *Journal of Chromatography. A*, vol. 1218, no. 49, pp. 8748–8759, 2011.

[13] X. Wang, W. Kong, W. Xie et al., "Bi-porous bioinspired chitosan foams with layered structure and their adsorption for xylenol orange," *Chemical Engineering Journal*, vol. 197, pp. 509–516, 2012.

[14] P. Mallika, A. Himabindu, and D. Shailaja, "Modification of chitosan towards a biomaterial with improved physico-chemical properties," *Journal of Applied Polymer Science*, vol. 101, no. 1, pp. 63–69, 2006.

[15] F. M. Plieva and B. Mattiasson, "Macroporous gel particles as novel sorbent materials: rational design," *Industrial and Engineering Chemistry Research*, vol. 47, no. 12, pp. 4131–4141, 2008.

[16] T. Y. Hsien and G. L. Rorrer, "Effects of acylation and cross-linking on the material properties and cadmium ion adsorption capacity of porous chitosan beads," *Separation Science and Technology*, vol. 30, no. 12, pp. 2455–2475, 1995.

[17] B. Zhang, X. Yang, P. Li, C. Guo, X. Ren, and J. Li, "Preparation of chitosan sulfate and vesicle formation with a conventional cationic surfactant," *Carbohydrate Polymers*, vol. 183, pp. 240–245, 2018.

[18] R. V. Rios, R. Garzón, S. C. S. Lannes, and C. M. Rosell, "Use of succinyl chitosan as fat replacer on cake formulations," *LWT*, vol. 96, pp. 260–265, 2018.

[19] M. Monier and D. A. Abdel-Latif, "Fabrication of Au(III) ion-imprinted polymer based on thiol-modified chitosan," *International Journal of Biological Macromolecules*, vol. 105, Part 1, pp. 777–787, 2017.

[20] Y. Yuan, Z. L. Wan, S. W. Yin et al., "Characterization of complexes of soy protein and chitosan heated at low pH," *LWT - Food Science and Technology*, vol. 50, no. 2, pp. 657–664, 2013.

[21] G. Li, J. Huang, T. Chen, X. Wang, H. Zhang, and Q. Chen, "Insight into the interaction between chitosan and bovine serum albumin," *Carbohydrate Polymers*, vol. 176, pp. 75–82, 2017.

[22] O. Masalova, V. Kulikouskaya, T. Shutava, and V. Agabekov, "Alginate and chitosan gel nanoparticles for efficient protein entrapment," *Physics Procedia*, vol. 40, pp. 69–75, 2013.

[23] H. Yi, L. Q. Wu, W. E. Bentley et al., "Biofabrication with chitosan," *Biomacromolecules*, vol. 6, no. 6, pp. 2881–2894, 2005.

[24] R. L. Machado, E. J. de Arruda, C. C. Santana, and S. M. A. Bueno, "Evaluation of a chitosan membrane for removal of endotoxin from human IgG solutions," *Process Biochemistry*, vol. 41, no. 11, pp. 2252–2257, 2006.

[25] A. Gamzazade, A. Sklyar, S. Nasibov, I. Sushkov, A. Shashkov, and Y. Knirel, "Structural features of sulfated chitosans," *Carbohydrate Polymers*, vol. 34, no. 1-2, pp. 113–116, 1997, 113.

[26] S. Dimassi, N. Tabary, F. Chai, N. Blanchemain, and B. Martel, "Sulfonated and sulfated chitosan derivatives for biomedical applications: a review," *Carbohydrate Polymers*, vol. 202, pp. 382–396, 2018.

[27] D. Guo, C. Lou, P. Zhang et al., "Polystyrene-divinylbenzene-glycidyl methacrylate stationary phase grafted with poly (amidoamine) dendrimers for ion chromatography," *Journal of Chromatography. A*, vol. 1456, pp. 113–122, 2016.

[28] A. Saxena, B. P. Tripathi, and V. K. Shahi, "An improved process for separation of proteins using modified chitosan–silica

cross-linked charged ultrafilter membranes under coupled driving forces: Isoelectric separation of proteins," *Journal of Colloid and Interface Science*, vol. 319, no. 1, pp. 252–262, 2008.

[29] D. Verma, M. S. Desai, N. Kulkarni, and N. Langrana, "Characterization of surface charge and mechanical properties of chitosan/alginate based biomaterials," *Materials Science and Engineering: C*, vol. 31, no. 8, pp. 1741–1747, 2011.

[30] O. I. Shchukina, A. V. Zatirakha, A. S. Uzhel, A. D. Smolenkov, and O. A. Shpigun, "Novel polymer-based anion-exchangers with covalently-bonded functional layers of quaternized polyethyleneimine for ion chromatography," *Analytica Chimica Acta*, vol. 964, pp. 187–194, 2017.

[31] L. S. Guinesi and É. T. G. Cavalheiro, "The use of DSC curves to determine the acetylation degree of chitin/chitosan samples," *Thermochimica Acta*, vol. 444, no. 2, pp. 128–133, 2006.